COLLOIDS AND SURFACES B-BIOINTERFACES (ISSN: 0927-7765) 122: 529-536 (2014)

doi:10.1016/j.colsurfb.2014.07.025

Surface Modification of HSA Containing Magnetic PLGA Nanoparticles by Poloxamer to Decrease Plasma Protein Adsorption

Quazi T. H. Shubhra[a,b*], *Judit Tóth*[b,c], *János Gyenis*[b], *Tivadar Feczkó*[b,c]

[a†]Doctoral School of Molecular and Nanotechnologies, Faculty of Information Technology, University of Pannonia, Egyetem u.10, H-8200 Veszprém, Hungary,

[b⊥]Research Institute of Chemical and Process Engineering, Faculty of Information Technology, University of Pannonia, Egyetem u.10, H-8200 Veszprém, Hungary,

[c‡]Institute of Materials and Environmental Chemistry, Research Centre for Natural Sciences, Hungarian Academy of Sciences, Pusztaszeri u. 59-67., H-1025 Budapest, Hungary

ABSTRACT

Lifetime prolongation for hydrophobic drug carriers has been the focus of interest for many years. Poloxamer (Pluronic F68, PF68) has been employed in this study for modifying the surface of magnetic poly(D,L-lactic-co-glycolic acid) (PLGA) nanoparticles (NPs) loaded with human serum albumin (HSA) model drug. Surface characteristics of untreated and PF68 treated NPs were analyzed by size, zeta potential and electrophoretic mobility studies. UV/VIS spectroscopic analysis, isothermal titration calorimetry (ITC) and dynamic light scattering methods were used to investigate serum protein (bovine serum albumin, BSA) adsorption. Results showed the successful surface attachment of PF68. Among different concentrations (0.1 to 1% wt/vol) of PF68 studied, 0.5% was found to be the most useful, since a higher concentration can issue in micelle formation. 50% less BSA tended to be adsorbed on the treated NPs in comparison to the untreated ones.

---

* Correspondence: shubhro.du@gmail.com; Fax:+36-88624038 ; Tel : + +3688623509.

KEYWORDS: poloxamer; protein adsorption; surface modification; isothermal titration calorimetry.

1. Introduction

Immobilized proteins/enzymes are currently the object of considerable interest, which involves attaching proteins/enzymes to a solid support. Immobilized enzymes have been playing a major role in modern biosensor technology, while immobilized antibodies are used to devise highly selective immunoassays for diagnostic purposes. Proteins can be immobilized on a solid support either chemically or physically [20]. Physical immobilization involves the entrapment of proteins inside semipermeable microcapsules or polymer lattices, or simple adsorption of proteins onto a solid surface. Chemical immobilization involves the formation of at least one covalent bond between the protein and the functionalized insoluble matrix. Chemical immobilization is by far more popular due to its better stability. For the covalent immobilization of proteins, NPs require activated chemical groups capable of reacting with primary amines or carboxylic acids, the two most available functional groups on the protein surface. Gold (Au) NPs or Au coated NP surfaces find interest in cancer treatment or diagnostics. For example, AuNPs are used as an absorber of X-rays for treating solid tumors or in photothermal therapy. Au surfaces can be modified easily by self-assembled monolayers (SAM) of thioalkyl derivatives. Native and fragmented anti-gp51 antibodies were immobilized on magnetic gold nanoparticles (MNP-Au) by Baniukevic et al. [21]. Due to the gold coating, magnetite NPs exhibit optical properties of Au metal in addition to the magnetic properties of Fe_3O_4. The developed surface-enhanced Raman scattering-based sandwich immunoassay was successfully applied for the detection of the bovine leukemia virus antigen gp51 in milk samples in a rapid, reliable and selective manner.

Biocompatible PLGA is extensively used for preparing nano/micro particles [1,2]. PLGA is a biocompatible and biodegradable polymer having FDA (Food and Drug Administration) approval, and very frequently used for the preparation of nano- and microparticles [3] with an excellent drug loading capacity. The adsorption of proteins to NP surfaces has become the subject of intense research for several decades. After being injected into the bloodstream, NPs are immediately covered by plasma proteins [4]. NP/protein(s) complexes are readily identified by the immune system [5,6]. As a result, NPs will be uptaken by cells of RES (reticuloendothelial system), especially the macrophages of the MPS (mononuclear phagocyte system) [7]. For hydrophobic NPs, this problem can be overcome by the proper modification of the surfaces with poloxamers [8]. Poloxamers are triblock copolymers having PPO (polypropyleneoxide) and PEO (polyethyleneoxide) blocks [9,10]. They can interact with hydrophobic particles, biological membranes, etc [11-13]. The structure of poloxamer and their adsorption pattern onto hydrophobic PLGA NPs are shown in Figure 1.

Many works and several reviews have been published in the last decade on the application of poloxamers for drug delivery. Kabanov et al. reviewed drug and gene delivery, and described poloxamer micelles and micellar drug formulations, drug release from micelles, and pharmacokinetic and biodistribution of poloxamers [14]. Batrakova et al. published a review on drugs and genes delivery using poloxamers [15]. Micellar formulations and unimer-associated biological response modifying effects of poloxamers were described in that study as showing exceptional potentiality of application in pharmaceutical industries. Multiple effects of poloxamers in multidrug resistant cells were also highlighted. Poloxamer excipients have been extensively used in

pharmaceutical industries as emulsifier, solubilizer for hydrophobic drugs and suspension stabilizer. They also find application in parenteral dosage forms. An intravenous formulation of poloxamer 188 is being marketed by the name RheothRx injection.

HSA is the most abundant plasma protein in the human body [16], and was selected as a model drug in this study. Oleic acid coated Fe_3O_4 is dispersible in many organic medium. Magnetite shows biological compatibility with FDA approval for clinical usage [17-19]. Particles containing magnetic cores can be manipulated by magnetic field or monitored by magnetic resonance imaging. For example, anionic magnetic nanoparticles have been used to adsorb and release cationic drugs for potential cancer immunotherapy.

The aim of this study was to modify the surface of PLGA nanoparticles by using PF68. PLGA NPs co-encapsulating HSA and magnetic NPs (magnetite), were prepared by double emulsion solvent evaporation method [1,3]. To the best of our knowledge, co-encapsulation of HSA along with Fe_3O_4 is rarely studied by other groups. The main challenges were the effective surface modification providing reduced protein adsorption, no agglomeration and a narrow size distribution having <220 nm size for enabling sterilization by ultrafiltration via a membrane with 220 nm cut-off value [22,23]. In the light of this size barrier, PLGA NPs of less than 150 nm were prepared compromising encapsulation efficiency after making a mathematical optimization using the GAMS^{TM}/MINOS software. The surfaces of prepared NPs were successfully modified with PF68 prioritizing the size barrier, and maintaining the size range up to <220 nm.

2. Materials and Methods

2.1 Materials

PLGA (50:50, M_w = 8000, Resomer® RG 502H) with free carboxyl end groups was supplied by Boehringer Ingelheim, Germany. BSA and HSA were obtained from Trigon Biotechnological Ltd., Hungary. The concentration of bulk HSA solution was 36.87 g/L. Dichloromethane (DCM) was purchased from Scharlab, Hungary. Polyvinyl alcohol (PVA, M_w = 30,000–70,000), poloxamer (Mw = 8350, BASF, Ludwigshafen, Germany, Pluronic® F68) and phosphate-buffered saline (PBS, pH 7.4) were products of Sigma-Aldrich, Germany. The micro-BCA (bicinchoninic acid) protein assay kit was purchased from Pierce Biotechnology, Inc., USA. Oleic acid coated magnetite was synthesized by co-precipitation method.

2.2 Synthesis of oleic acid-coated superparamagnetic iron oxide nanoparticles

Neat superparamagnetic oleic acid coated iron oxide NPs were prepared by co-precipitation of Fe(II) and Fe(III) chlorides in an aqueous ammonia solution. The detailed process can be found in our previously published paper [1]. The size of magnetite was 10 ± 5 nm.

2.3 Process parameters and optimization

Performing some preliminary tests, five process variables (factors F1–F5) have been found to strongly influence the hydrodynamic particle sizes and/or the encapsulation process. Process optimization (using software GAMS™/MINOS) was discussed in our previously published paper [2]. The list of process variables and the optimum condition used for this study is given in Table 1.

2.4 Preparation of PLGA nanoparticles

Nanoparticles were prepared by double emulsion solvent evaporation method [2,23]. The detailed preparation process can be found in our previously published paper [1]. Briefly, PLGA was dissolved in solvent DCM. Fe_3O_4 was added to the system and dispersed using a probe sonicator (Model W-220 probe sonicator, Heat Systems-

Ultrasonics). The power of sonication was 70 W, frequency was 20 kHz. Then 0.5 ml model drug solution of preset concentration, diluted with PBS, was added to the system and the two-phase system was emulsified for 60 s. This emulsion was dispersed in 2 wt% aqueous PVA to obtain w/o/w double emulsion. The DCM was evaporated to solidify PLGA NPs under continuous stirring (800 rpm) for 2 h using a magnetic stirrer. After the evaporation of DCM, dispersed solid PLGA NPs with encapsulated model drug and Fe_3O_4 were obtained and stored for further experimental analysis.

2.5 Redispersion of PLGA NPs

Nanoparticles were redispersed in distilled water using probe sonicator after ultracentrifugation (Beckman Coulter Optima^{TM} MAX-E ultracentrifuge, USA). The ultracentrifugation was carried out for 50 minutes at 10°C using the speed 50,000 rpm.

2.6 Surface functionalization of PLGA NPs

Poloxamers readily dissolve in water. Poloxamer solutions of different concentrations (PF68 0.1, 0.25, 0.5, 0.75 and 1% wt/vol) were prepared by simply dissolving them in distilled water and were used to coat the PLGA NPs that were redispersed in distilled water before the addition of PF68.

2.7 Hydrodynamic size, ζ-potential and electrophoretic mobility measurement

The size of the NPs was analyzed by dynamic light scattering (DLS) method (also called as photon correlation technique) using Zetasizer Nano ZS (Malvern Instruments, Malvern, UK) at 25°C. For each sample, five parallel size measurements were carried out and the mean of the five measurements was calculated. The ζ-potential and electrophoretic mobility were measured using the same Zetasizer Nano ZS at 25°C.

2.8 Protein adsorption studies

BSA was dissolved in distilled water and then added to the NP suspension (unmodified) and dispersion (modified). 5 ml portions of NP suspension (1.19 mg/ml PLGA) was mixed with 4 ml BSA solution (0.1 mg/ml) for 2 h using magnetic stirrer. The obtained solution was then kept overnight in the refrigerator to allow more time for the protein to be adsorbed on NPs. After ultracentrifugation, the degree of protein

adsorption was determined indirectly by analyzing the non-adsorbed portion with UV/VIS spectrometry using micro BCA protein assay kit at the wavelength of 562 nm.

The adsorption was also examined by measuring and comparing the size and the zeta potential of the modified and unmodified NPs using Zetasizer Nano ZS.

Finally, an isothermal titration calorimeter VP-ITC (MicroCal, Northampton, MA) was used to investigate the protein adsorption. The concentrations of NPs and BSA were 1.19 mg/ml (wt/vol) and 10 mg/ml (wt/vol), respectively. The modified and the unmodified samples and BSA were dialyzed against PBS at 4°C, thoroughly degassed by stirring under vacuum before sampling for the titration. 200 μL suspension of modified and unmodified PLGA NPs were loaded into the titration cell, respectively. 280 μL BSA was loaded into the injection syringe from which 20 μL was introduced to the titration cell during every injection. The temperature of the titration cell was fixed at 25°C. The single injection method (SIM) was also applied for both modified and unmodified PLGA NPs to confirm the result obtained by multiple injections. MicroCal Origin software was used to analyze the data.

3. Results

3.1 The surface charge of PLGA NPs

The PLGA used in this study has free carboxyl end groups and forms a negatively charged surface in the aqueous solution (Figure 2a). This was also confirmed by electrophoretic mobility (μ) study which was measured as a function of the pH of the medium (Figure 2b). The pH changes were made by the addition of dilute HCl and NaOH. In all cases the μ values sharply increased when the pH changed to more acidic pH values (from 6 to 3), whereas more constant values were observed at basic pHs (from 8 to 10), which is in agreement with the study of Ortega et al [13].

3.2 Surface attachment of poloxamer

The surface attachment of PF68 was confirmed by size and zeta potential (ZP) studies. The increase in size and change in ZP values obtained indicated the surface attachment of PF68 on PLGA NPs. The size and ZP values of control PLGA NPs and PF68 treated PLGA NPs are shown in Table 2.

It was found that with the increase in poloxamer concentration, the size distributions of PF68 coated PLGA NPs shifted toward the higher particle size region with significant simultaneous increase in the volume mean particle size. The increase was sharp and high for up to 0.5% poloxamer concentration, however, above that concentration, it was quite steady (Table 2).

3.3 Protein adsorption

Equation (1) was used to calculate protein adsorption from the amount of protein left in the supernatant and the total amount of protein added initially.

$$\%\ BSA\ adsorbed\ = \frac{(m_{BSA_{\text{int}}} - m_{BSA_{\text{supernatant}}})}{m_{BSA_{\text{int}}}} \times 100\% \qquad (1)$$

where m_{BSAint} = total amount of the introduced BSA (mg) and $m_{BSAsupernatant}$ = total amount of BSA in the supernatant (mg).

For both untreated and PF68 treated PLGA NPs, the absorbance of reference samples (without BSA) was measured and subtracted from the total absorbance of samples since disturbance is expected due to the presence of residual PVA and non-encapsulated model drug.

Figure 3 shows the percentage of protein adsorbed for both treated and untreated PLGA NPs. To substantiate the result of protein adsorption shown in Figure 3, size and ZP analysis were carried out (Table 3).

3.4 Isothermal calorimetric analysis

The protein binding energetics for BSA adsorption onto untreated and 0.5% PF68 treated PLGA NPs were studied using the isothermal titration calorimetry (Figure 5). The observed heat effects indicated a definite interaction between BSA and NPs. The one-site model was used to fit the data (lower panels in Figure 5).

Adsorption of BSA on NP surfaces is spontaneous and Gibbs free energy (ΔG) is negative. For untreated NPs, heat release (ΔH) is lower than for treated ones and entropy

change is also favorable indicating that the process is entropy driven involving primarily hydrophobic interactions. Larger heat release (ΔH) and unfavorable entropy change (-TΔS is positive) for treated samples indicate that the process is enthalpy driven involving hydrogen bonding in addition to hydrophobic interactions [24].

Although before the experiments it was expected that more protein adsorption would show larger peaks and occupy more area in raw ITC figure for treated NPs, the obtained result was the opposite. To confirm the finding, the single injection method (SIM) was also applied. The result shown in Figure 8 clearly shows a larger exothermic peak for treated NPs indicating a high heat release due to the H-bonding which is in agreement with the result shown in Figure 5.

4. Discussion

The PLGA used in this study was negatively charged due to the existence of the free carboxyl end group. The addition of acid starts to minimize surface negativity, and between pH 4 and 5 the surface does not have net charge, which is the isoelectric point. The further addition of acid results in the accumulation of positive charges on the surface providing positive zeta potential.

The surface attachment of PF68 was confirmed by size and ZP studies. The volume mean size of our control sample was 142 nm and for coating with 1% PF68, almost 50 nm enhancement in size was observed which is comparable to the result obtained by Greenwood [25]. Since due to the poloxamer coating one peak remained in the size distribution (not shown), we assumed that all of the size increment was the result of the poloxamer coating. However, it cannot be excluded that poloxamer-assisted particle growth of some smaller particles could occur.

Ortega et al. [26] found a sharp increase in the adsorption isotherm of PF68 coated PLGA particles for low PF68 concentration (up to 100 mg/L), whilst above that value, the increase was quite steady, and reached a plateau, which supports our findings . If the number of poloxamer attached is higher, the surface is highly crowded, consequently, adlayer thickness increases [27]. With the increase in concentration of PF68, micelle formation appears followed by micellar aggregation [28]. Considering the

problem of micelle formation and aggregation, 0.5% PF68 was selected for PLGA NP treatment and used for further analysis in this study. Moreover, the size of 0.5% PF68 treated NPs is about 40 nm below the membrane cut-off value, which will be used for ultrafiltration as mentioned in the introduction part. Absolute differences in ZP values should be at least 10 mV to allow the prediction of distinct stability [29]. The treated PLGA NPs were fairly more stable even after few days of treatment showing comparatively little sedimentation, which can be clearly observed by the naked eyes and is also supported by the ZP values shown in Table 2. On the other hand, the control sample forms observable coagulates or flocculates after a few hours of preparation which increases with time. This is also supported by our ZP values shown in Table 2. In all cases, visual observation strongly supported the ZP values obtained in this study. The addition of poloxamer leads to an increase in surface negativity.

The protein adsorption can be reduced to almost 50 % by treating PLGA NPs with PF68 (Figure 3). The comparison of this result with other published results is not so easy since protein adsorption depends on the type of protein and the surface charge of NPs. From Table 2, it can be understood that the PLGA NPs studied have high negative ZP values indicating high number of negative charges on the NP surface. From Table 3, it is clear that BSA adsorption increases the size and decreases the ZP of the control sample significantly in comparison to the treated sample, which indicates that less protein was adsorbed on treated NPs supporting results of Figure 3.

The adsorption of BSA to the negatively charged PLGA surface is somewhat puzzling since the isoelectric point of BSA is 4.6, and therefore BSA is negatively charged at pH 7 [30]. The adsorption mechanism is quite interesting and is explained schematically by the Figure 4. Aspartic acid and glutamic acid in BSA are negatively charged due to the presence of side chains with carboxylate groups. BSA also contains slightly positively charged amino acids, namely lysine and arginine [31,32]. Lysine has a side chain amino group, which can become positive by accepting a proton from water and arginine has a protonated guanidinium group. The net charge shown by BSA at pH 7 is negative as mentioned above. Although BSA undergoes conformational changes on the PLGA surfaces (described in the next subsection), the positively charged amino acids will be closer to the negatively charged PLGA surface than the negatively charged amino

acids like aspartic and glutamic acids. The negative PLGA surface will repel negative amino acids to take them away from the surface as far as possible whereas they will pull and attract the positively charged amino acids as close to the surface as possible (Figure 4b). It is also confusing that BSA which has net negative charge reduces the surface negativity (Table 3). From Figure 4, it can be understood that when BSA is adsorbed on PLGA, positively charged amino acids will be close to PLGA surface e.g. positive arginine. Hence, it can be considered that the positively charged amino acids will cover the surface reducing the surface negativity of PLGA showing lower ZP values.

Protein adsorption is a very complicated process. Hydrophobic interaction is the main mechanism for protein adsorption on hydrophobic surfaces. Electrostatic interaction is observed for protein adsorption on hydrophilic surfaces, which is unfavorable but not impossible for hydrophobic surfaces. BSA is charged protein and charged amino acids are hydrophilic. They exist on the surface of a protein interacting with the surrounding water keeping the hydrophobic amino acids away from the water. Thus, for BSA, the charged amino acids are on the water side (opposite to the PLGA NP surface), whereas the hydrophobic amino acids are located close to the NP surfaces leading to BSA adsorption on NP surfaces. Since, hydrophilic charged groups can be on the water side, hydrogen bond between the BSA and the PLGA is not expected. Due to hydrophobic interaction between protein and hydrophobic PLGA, entropy gain is observed (from Figure 5, it is 6.1 cal/mol/deg), which is due to the release of water molecules from the hydrophobic surface. "Soft" proteins like BSA show conformational change (Figure 6) when adsorbed onto hydrophobic particles [33].

Poloxamers are surfactants and readily dissolve in water forming strong hydrogen bonds with water. It is expected and from Figure 5 can be assumed that hydrogen bond will be formed between the BSA and the poloxamer, since both of them are hydrophilic. The H-bond formation will release heat to a greater extent than a simple hydrophobic interaction between BSA and PLGA NPs, as can be seen from Figure 5 (ΔH is significantly higher for treated nanoparticles than that for untreated one). The scheme in Figure 7 shows how lysine and arginine of BSA can form H-bonds with poloxamer.

This result is novel and is not easy to compare with other published work due to the incorporation of model drug (HSA) and oleic acid coated magnetite. The interaction

of poloxamer and PLGA have already been examined by ITC, but NPs containing PLGA, poloxamer, HSA and oleic acid coated magnetite have not been studied before. Iseult et al. investigated the binding of protein HSA (human serum albumin) to hydrophobic polymeric NPs with and without oleic acid [34]. Very different interaction patterns were observed in the presence and absence of oleic acid. The hydrophobic NP-HSA interaction was exothermic in the absence of OA, whereas the presence of OA gave endothermic signal. This study gives an idea that the presence of other molecules/ions can affect the heat release pattern during the ITC analysis and can even change the release pattern from exothermic to an endothermic one.

5. Conclusion

The poloxamer coating makes hydrophobic carriers "stealth", hence they can reach the target site(s), where they can perform their biological roles. Size and zeta potential results showed that poloxamer adsorbed on the studied magnetic PLGA NPs. For all of the studied concentrations of poloxamer, sharp changes in both size and ZP values were obtained. The mean size of unmodified NPs was 142 nm whereas for 0.5 and 1% PF68 modified NPs, the values were 177 and 191 nm, respectively. ITC analysis indicated mainly hydrophobic interactions between BSA and unmodified PLGA NPs whereas H-bonds formed between PF68 and BSA. For modified NPs the decrease in ZP values (-42 to -34 mV) was significantly lower than that for modified NPs (-36 to -24 mV) indicating less protein adsorption on the surface of modified PLGA NPs which in turn showed the effective surface modification. UV/VIS spectrophotometric analysis using micro-bicinchoninic acid protein assay indicated a 50% reduction in protein adsorption after PLGA NPs modified with 0.5% PF68. The reduced protein adsorption can contribute to keeping the HSA loaded NPs in the bloodstream for prolonged period.

Acknowledgements

We thank Prof. Ferenc Vonderviszt for instrumental support in the ITC analysis. The authors acknowledge the financial support of the European Commission granted

through the “PowTech” Marie Curie Initial Training Network (Grant Agreement No: 264722).

Abbreviations

BSA = bovine serum albumin

HSA = human serum albumin

ITC = isothermal titration calorimetry

MPS = mononuclear phagocyte system

NP = nanoparticle

PEO = polyethyleneoxide

PLGA = poly(D,L-lactic-co-glycolic acid)

PPO = polypropyleneoxide

RES = reticuloendothelial system

ZP = zeta potential

6. References

[1] Q.T.H. Shubhra, A.F. Kardos, T. Feczkó, H. Mackova, D. Horák, J. Tóth, G. Dósa, J. Gyenis, J. Microencapsul. 31 (2014) 147-155.

[2] Q.T.H. Shubhra, T. Feczkó, A.F. Kardos, J. Tóth, H. Mackova, D. Horák, G. Dósa, J. Gyenis, J. Microencapsul. 31 (2014) 156-165.

[3] Q.T.H. Shubhra, H. Macková, A.F. Kardos, D. Horák, J. Tóth, J. Gyenis, T. Feczkó, e-Polym. 13 (2013) 310–318.

[4] N. Welsch, Y. Lu, J. Dzubiella, M. Ballauff, Polymer, 54 (2013) 2835-2849.

[5] A.J. Andersen, S.H. Hashemi, T.L. Andresen, A.C. Hunter, S.M. J. Biomed. Nanotechnol. 5 (2009) 364–372.

[6] G. Borchard, J. Kreuter, Pharm. Res. 13 (1996) 1055–1058.

[7] K. Sempf, T. Arrey, S. Gelperina, T. Schorge, B. Meyer, M. Karas, J. Kreuter, Eur. J. Pharm. Biopharm. 85 (2013) 53–60.

[8] Q.T.H. Shubhra, T. Feczkó, J. Tóth, J. Gyenis, Polym. Rev. 54 (2014) 112-138.

[9 G.M. Walker, S.E.J. Bell, K. Greene, D.S. Jones, G.P. Andrews, Chem. Eng. Sci. 64 (2009) 91–98.

[10] W. Zou, C. Liu, Z. Chen, N. Zhang, Int. J. Pharm. 370 (2009) 187-195.

[11] M. Brigante, P.C. Schulz, J. Surfactants Deterg. 14 (2011) 439-453.

[12] D. Mustafi, C.M. Smith, M. W. Makinen, R.C. Lee, Biochim. Biophys. Acta. 1780 (2008) 7-15.

[13] M.J. Santander-Ortega, N. Csaba, M.J. Alonso, J.L. Ortega-Vinuesa, D. Bastos-González, Colloid. Surfaces A. 296 (2007) 132-140.

[14] A.V. Kabanov, E.V. Batrakova, V.Y. Alakhov, J. Control. Release 82 (2002) 189-212.

[15] E.V. Batrakova, A.V. Kabanov, J. Control. Release 130 (2008) 98-106.

[16] F. Yang, C. Bian, L. Zhu, G. Zhao, Z. Huang, M. Huang, J. Struct. Biol. 157 (2007**)** 348–355.

[17] R. Weissleder, D.D. Stark, B.L. Engelstad, B.R. Bacon, C.C. Compton, D.L. White, P. Jacobs, J. Lewis, Am. J. Roentgenol. 152 (1989) 167-173.

[18] R.H. Müller, S. Maaβen, H. Weyhers, F. Specht, J.S. Lucks, Int. J. Pharm. 138 (1996) 85–94.

[19] A. Ibrahim, P. Couvreur, M. Roland, P. Speiser, J. Pharm. Pharmacol. 35 (1983) 59-61.

[20] C. Duan, M.E. Meyerhoff, Microchimica Acta 117 (1995) 195-206.

[21] J. Baniukevic, I.H. Boyaci, A.G. Bozkurt, U. Tamer, A. Ramanavicius, A. Ramanaviciene, Biosens Bioelectron 43 (2013) 281–288.

[22] T. Feczkó, J. Tóth, G. Dósa, J. Gyenis, Chem. Eng. Process. 50 (2011) 846–853.

[23] T. Feczkó, J. Tóth, J. Gyenis, Colloid. Surface. A. 319 (2008) 188–195.

[24] E. Edink, C. Jansen, R. Leurs, I.J.P. de Esch, Drug Discov. Today. 7 (2010) 189–201.

[25] R. Greenwood, P.F. Luckham, T. Gregory, Colloid. Surface. A. 98 (1995) 117-125.

[26] M.J. Santander-Ortega, A.B. Jodar-Reyes, N. Csaba, D. Bastos-Gonzalez, J.L. Ortega-Vinuesa, J. colloid interf. Sci. 302 (2006) 522-529.

[27] S. Stolnik, N.C. Felumb, C.R. Heald, M.C. Garnett, L. Illum, S.S. Davis, Colloid. Surface. A. 122 (1997) 151-159.

[28] K. Garala, P. Joshi, M. Shah, A. Ramkishan, J. Patel, Int. J. Pharm. Invest. 3 (2013) 29–41.

[29] G.W. Lu, P. Gao, in V.S. Kulkarni (Ed), Handbook of Non-Invasive Drug Delivery Systems: Science and Technology, Elsevier, California, 2010, Chapter 3.

[30] S.H. Brewer, W.R. Glomm, M.C. Johnson, M.K. Knag, S. Franzen, Langmuir. 21 (2005) 9303-9307.

[31] K. Rezwan, L.P. Meier, L.J. Gauckler, Biomaterials. 26 (2005) 4351–4357.

[32] D.R. Persaud, A. Barranco-Mendoza, Food Chem. Toxicol. 42 (2004) 707–714.

[33] K. Nakanishi, T. Sakiyama, K. Imamura, J. Biosci. Bioeng. 91 (2001) 233–244.

[34] I. Lynch, K.A. Dawson, Nanotoday. 3 (2008) 40–47.

Table 1. Process variables (factors) and their optimum values.

Factor	Symbol	Variable	Optimum value
F1	X_{Fe3O4}	Fe_3O_4/PLGA weight ratio	**1 wt%**
F2	X_{PLGA}	PLGA concentration in the organic phase	**1 wt%**
F3	X_{HSA}	HSA concentration in the inner aqueous phase	**0.74 wt%**
F4	X_{VOLR}	Outer aqueous (w_2)/organic phase (o) volume ratio.	**2 vol/vol**
F5	$\boldsymbol{X_{time}}$	**Time of the ultrasonic treatment in the second emulsification**	**3 minutes**

Table 2. Average size and zeta potential of uncoated and PF68 coated PLGA NPs.

Percentage of PF68	Size (nm)	Zeta potential (mV)
0% (control)	142	-35
0.1% PF68	165	-43.8
0.25% PF68	167	-45.2
0.5% PF68	177	-49
0.75% PF68	181	-49.5
1% PF68	191	-53.9

Table 3. Size and ZP values of treated and untreated sample before and after protein adsorption.

Sample	Size (nm)		ZP (mV)	
	Before BSA adsorption	After BSA adsorption	Before BSA adsorption	After BSA adsorption
Control	157.5	183.26	-35.8	-24
0.5% PF68 treated	172.53	180.22	-42.1	-34.47

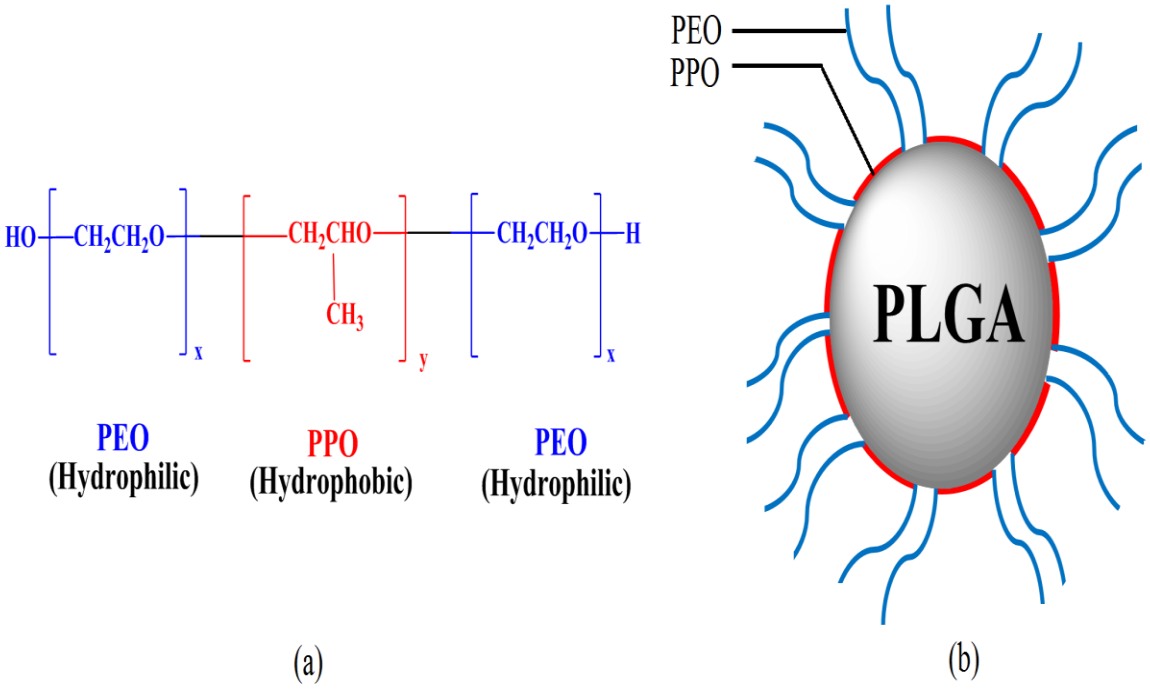

Figure 1. (a) Structure of poloxamer, (b) adsorption pattern of poloxamer (simple brush type) onto a PLGA NP.

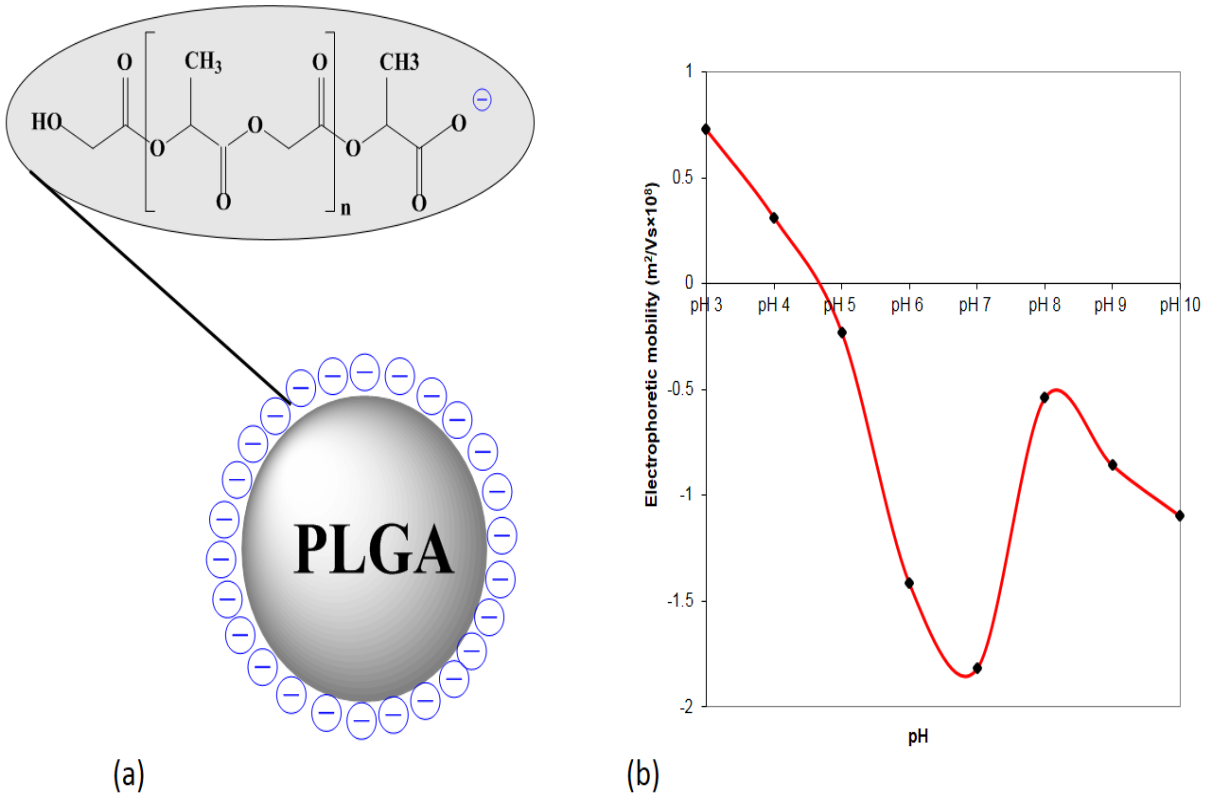

Figure 2. (a) Negatively charged PLGA NP (b) electrophoretic mobility (μ) as a function of pH.

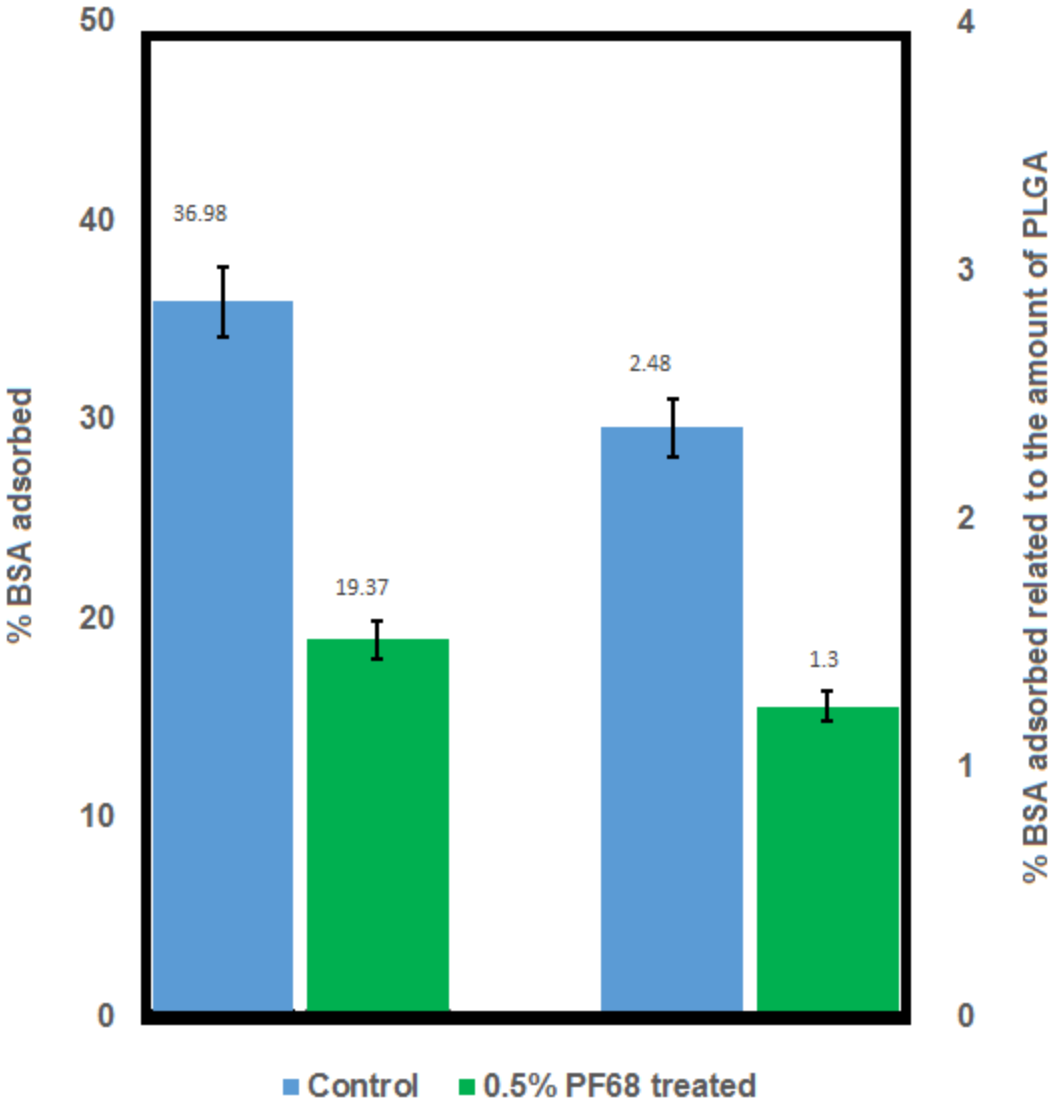

Figure 3. Percentage of BSA adsorbed for untreated and treated PLGA NPs.

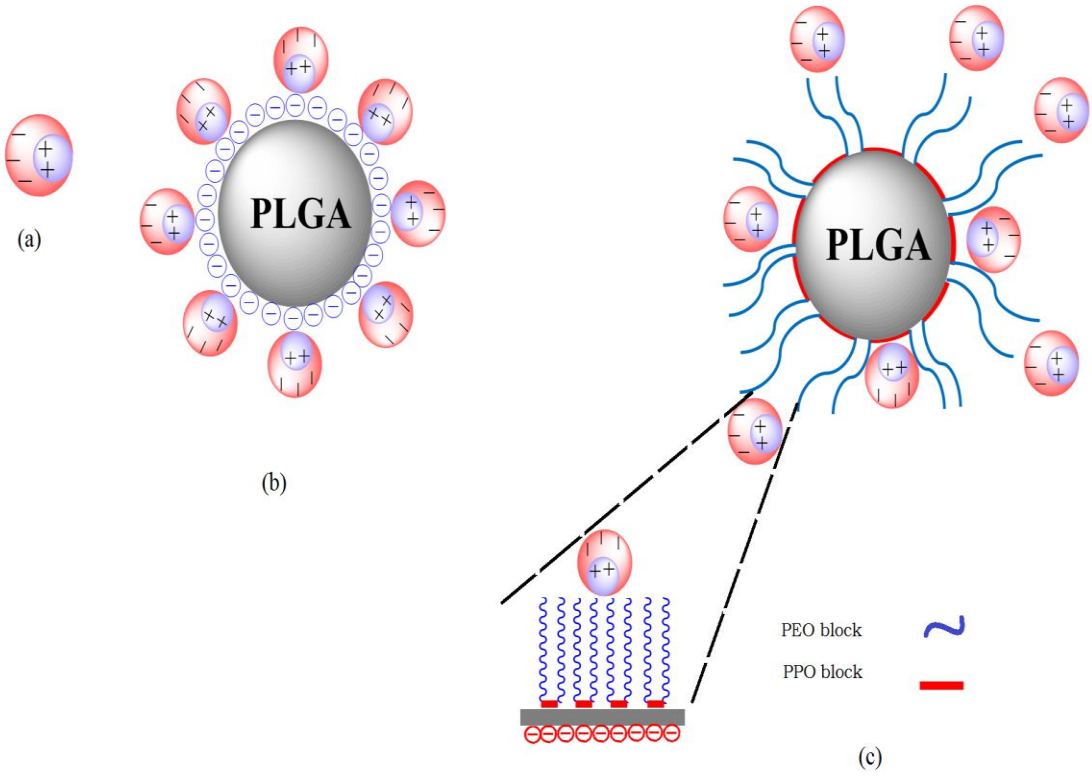

Figure 4. (a) BSA protein having net negative charge (light blue and light red color regions carry local net positive and negative charges, respectively), (b) adsorption of BSA onto a untreated PLGA NP and (c) prevention of protein adsorption onto PLGA NP by PF68 coating.

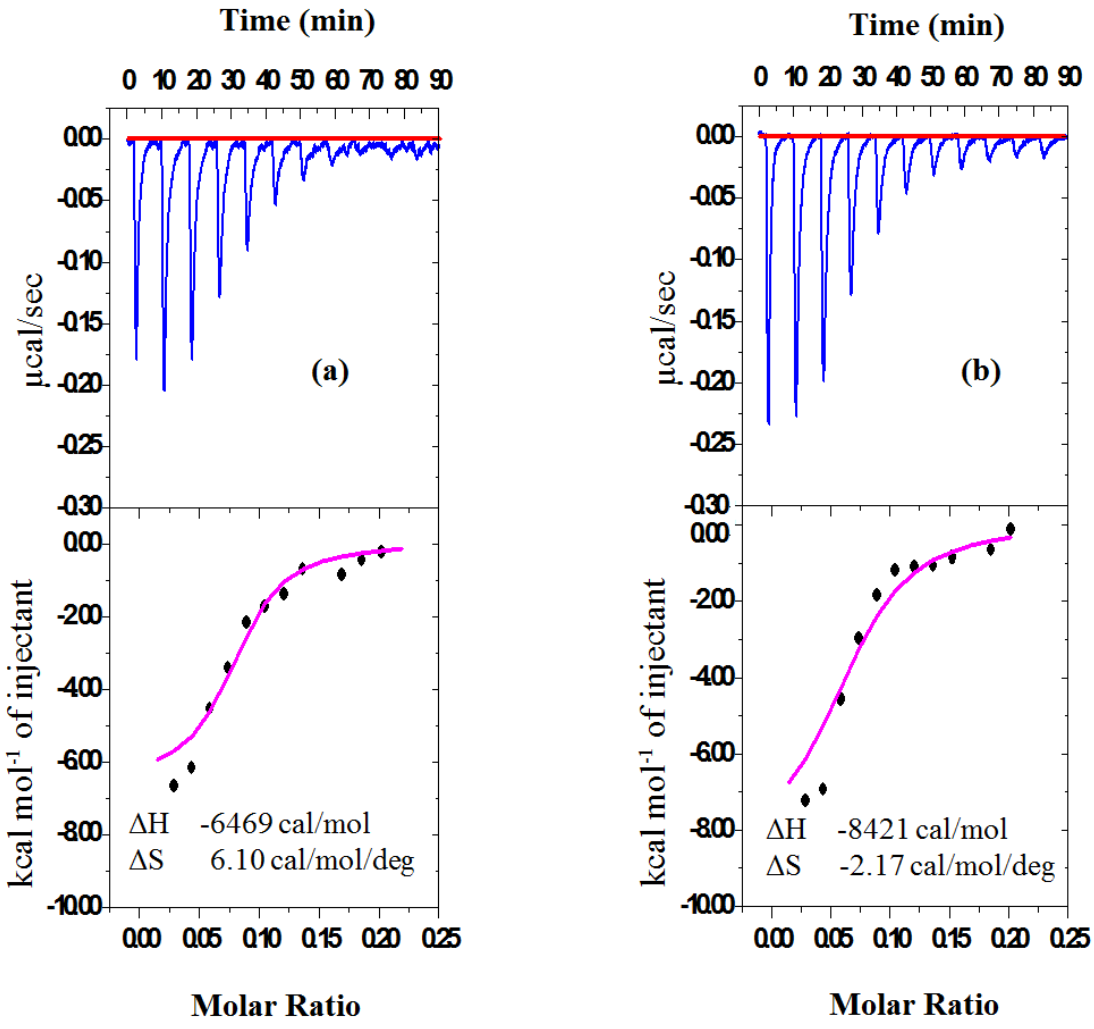

Figure 5. Calorimetric data (top panel: raw data; bottom panel: binding isotherms) for BSA adsorption onto (a) untreated PLGA NPs and (b) treated PLGA NPs.

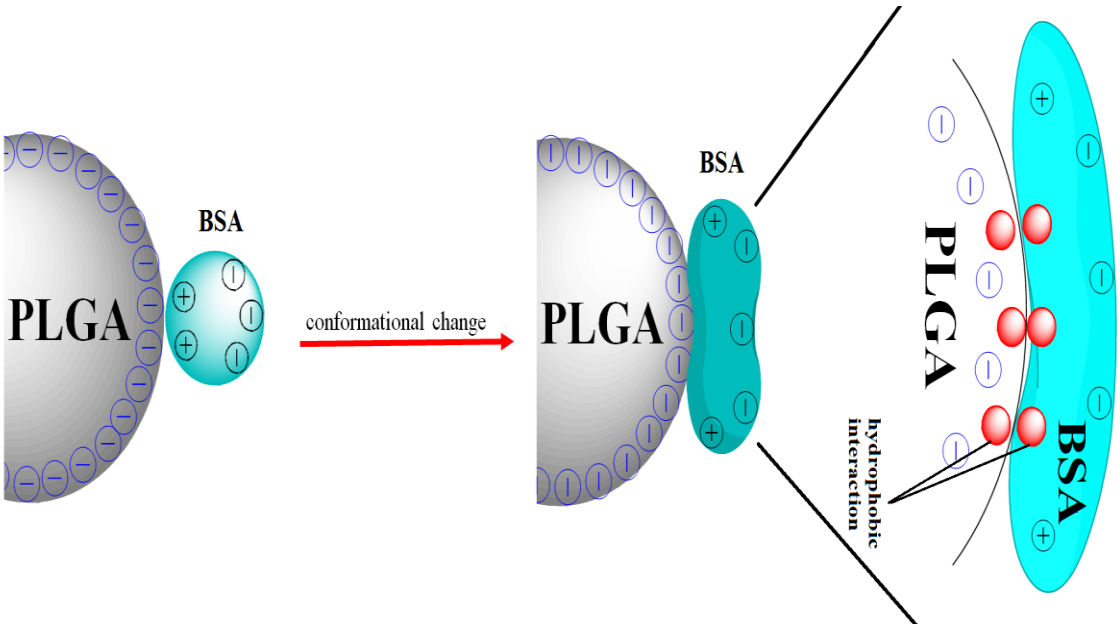

Figure 6. Soft protein adsorption on a hydrophobic PLGA NP.

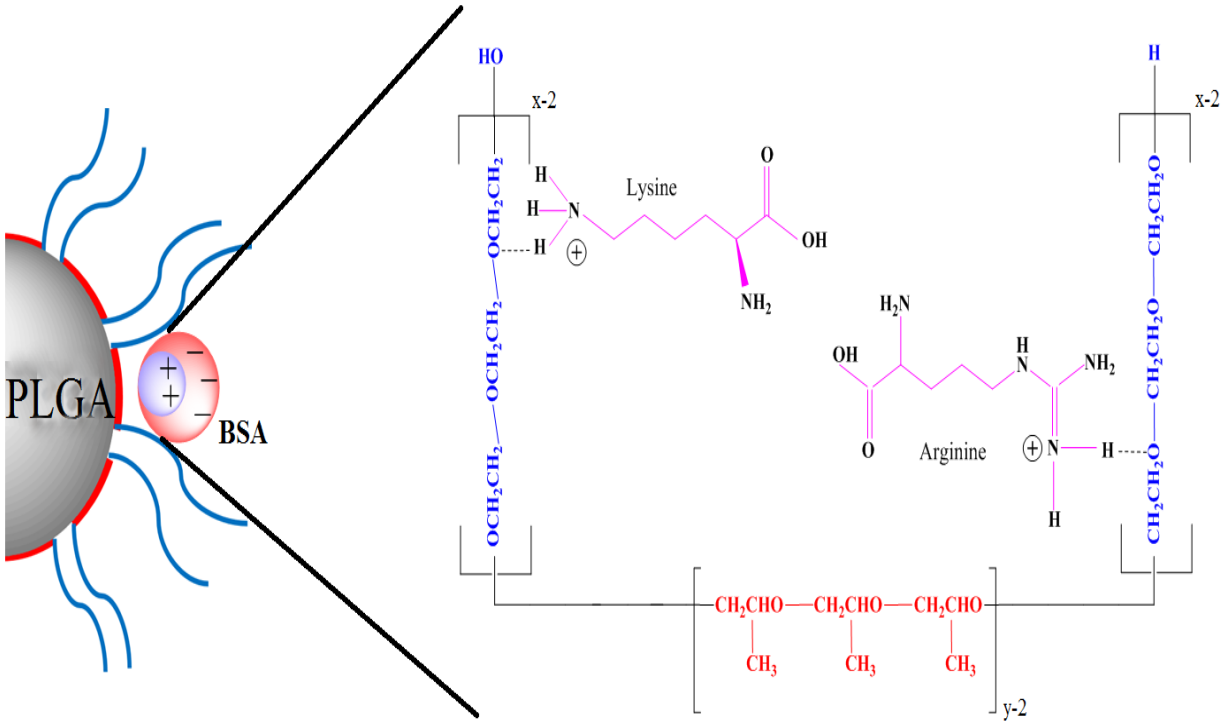

Figure 7. Hydrogen bonding between poloxamer and amino acids of BSA.

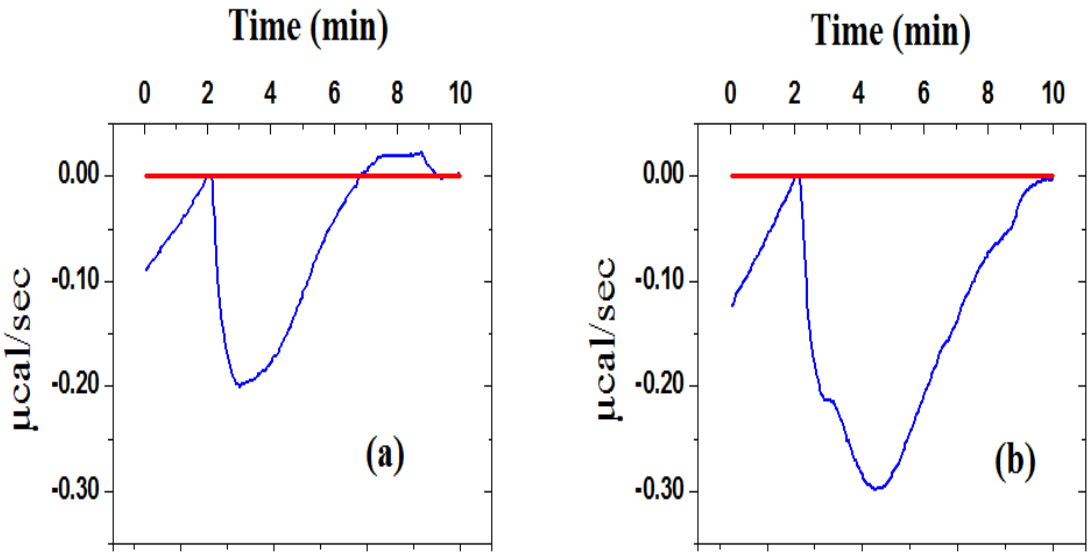

Figure 8. Raw ITC data using single injection method for BSA adsorption onto (a) untreated PLGA NPs and (b) treated PLGA NPs.